Evidence for enhanced Mediterranean thermohaline circulation during rapid climatic coolings

Isabel Cacho [a,d,1,*], Joan O. Grimalt [a], Francisco J. Sierro [b],
Nick Shackleton [c], Miquel Canals [d]

[a] *Department of Environmental Chemistry, Institute of Chemical and Environmental Research (CSIC),
Jordi Girona, 18, 08034-Barcelona, Catalonia, Spain*
[b] *Department of Geology, Faculty of Sciences, University of Salamanca, 37008-Salamanca, Spain*
[c] *University of Cambridge, The Godwin Laboratory, Pembroke Street, Cambridge CB2 3SA, UK*
[d] *G.R.C. Marine Geosciences, Department of Stratigraphy and Paleontology, University of Barcelona,
08071-Barcelona, Catalonia, Spain*

Abstract

Molecular biomarkers (C_{37} alkenones, *n*-nonacosane and *n*-hexacosanol) and TOC are used together with benthic $\delta^{18}O$ and $\delta^{13}C$ data to document the hydrographic response of the western Mediterranean Sea to rapid climatic variability. These proxies are recorded in core MD 95-2043 (Alboran Sea) affording the study of the Dansgaard–Oeschger (D–O) and Heinrich (HE) variability during the last glacial period. The results suggest that rapid changes in the western Mediterranean thermohaline circulation occurred in parallel to sea surface temperature oscillations. Enhanced deep water ventilation occurred during cold intervals (HE and D–O Stadials) probably driven by a strengthening of north-westerly wind over the north-western Mediterranean Sea. In contrast, decreased intensity of the thermohaline circulation is detected during warm intervals (D–O Interstadials) which led to low oxygenated deep water masses and better preservation of the organic matter in the sediment. © 2000 Elsevier Science B.V. All rights reserved.

Keywords: Heinrich events; Mediterranean Sea; biomarkers; deep-water environment; thermohaline circulation

1. Introduction

The climate of the last glacial period was very unstable. This characteristic was first reported in Greenland ice cores where the D–O cycles were

* Corresponding author.

[1] Present address: University of Cambridge, The Godwin Laboratory, Pembroke Street, Cambridge CB2 3SA, UK.

defined [1–3]. Further studies have demonstrated that a D–O-type variability also modulated the glacial climatology and hydrology of several other regions in the Northern Hemisphere ([4–6] and references therein). This rapid millennial-scale climatic variability suggests a rapid coupling of the atmospheric–oceanic systems.

The Mediterranean Sea is a semi-enclosed basin, extending W–E at intermediate latitudes ($\sim 30–45°N$). It operates as a concentration basin and the formation of dense water masses is driven

by climatic conditions [7,8]. In this context, climate signals are less attenuated being recorded in the sediments at much higher resolution than in the open ocean [9]. A recent, high resolution reconstruction of sea surface temperature (SST) in the Alboran Sea shows a D–O-type variability during the last ice age [5]. However, the impact of the abrupt climatic changes documented in Greenland ice core records on Mediterranean hydrography still remains to be explained.

The present study is focused on the analysis of some marine (C_{37} alkenones) and terrestrial (*n*-nonacosane and *n*-hexacosanol) biomarkers, TOC, benthic $\delta^{18}O$ and $\delta^{13}C$ on the time interval between 20 and 52 kyr BP in a long piston core from the Alboran Sea (MD 95-2043). The C_{37} alkenones are major components of haptophyteae algae from which the coccolithophore *Emiliania huxleyi* is the most abundant contributor at present day [10,11]. Their occurrence in ancient sediments is currently assumed to reflect contributions from algal primary productivity [12–14]. *n*-Nonacosane and *n*-hexacosanol are major lipid components of higher plant epicuticular waxes [15] and their concentration in marine sediments is widely used to record higher plant inputs to the marine environment [16,17]. The results are compared with the $U_{37}^{K'}$-SST and planktonic $\delta^{18}O$ profiles previously reported [5]. They provide a high resolution record of the rapid hydrographic changes of the western Mediterranean basin, responding to the D–O and HE variability.

2. Climatological and oceanographic setting

The Mediterranean Sea is located in a transitional climatic regime. In summer, it is dominated by the strong Azores anticyclone while in winter this high-pressure system collapses and European depressions migrate southwards creating high instability and frequent incursions of north-westerlies [18]. The predominant anticyclonic conditions produce an excess of evaporation over precipitation plus river runoff generating dense water masses [8,19]. Accordingly, this semi-enclosed sea is characterized by a complete thermohaline circulation system, involving surface water entrance from the north Atlantic Ocean, in situ densification by air–sea interaction and deep outflowing to the Atlantic.

Deepening of dense Mediterranean water masses occurs in three main vertical circulation belts [20]. Strong winter evaporation in the eastern basin generates levantine intermediate water (LIW) whereas deep water is produced in the Adriatic Sea (E Mediterranean) and the Gulf of Lions (W Mediterranean). These deep water systems operate similarly to the north Atlantic deep water overturning. LIW is also involved in the formation of deep water masses in both Adriatic and Gulf of Lions regions implying a strong communication between eastern and western basins at the level of these two deep overturning cells [20].

The Alboran Sea is the westernmost basin of the Mediterranean Sea and therefore, the first receiving inflowing Atlantic water. Three different water masses fill this basin whose circulation patterns are mainly controlled by water exchange through the narrow and shallow Strait of Gibraltar. The upper layer (0–220 m) is formed by modified Atlantic water (MAW) which flows eastwards through the Alboran Sea, describing two anticyclonic, western and eastern, gyres [21]. This surface water circulation pattern displays a high annual-interannual variability driven mainly by the position of the atmospheric pressure cells [21–25]. The second water layer (220–1100 m) is filled by LIW partially modified through its way from the eastern Mediterranean basin. This intermediate water mass is the main source of Mediterranean outflowing water (MOW) [26–28]. The deep layer (below 1100 m) is filled by western Mediterranean deep water (WMDW), which only contributes episodically (about 10%) to MOW [26,29,30].

2.1. Formation of Western Mediterranean Deep Water (WMDW)

The Gulf of Lions (Fig. 1) is one of the few oceanic regions where a deep water mass forms at present [31–33]. The production of deep water is controlled by wind strength, the initial density of the source waters (MAW and LIW), and the circulation pattern in the area. The latter consists of a large permanent cyclonic gyre, involving a
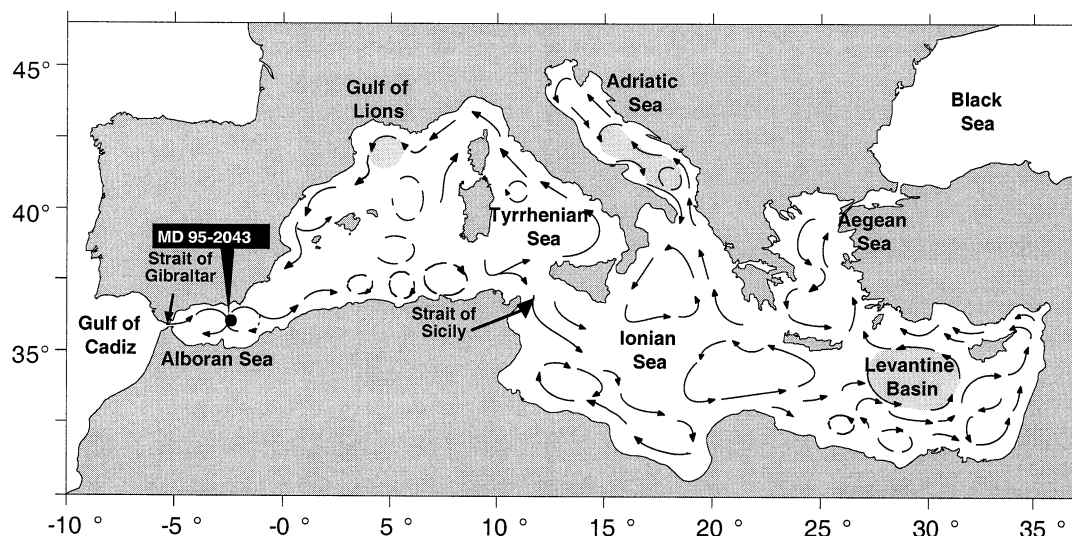
Fig. 1. Map of the Mediterranean Sea indicating the location of the studied core (MD 95-2043) and the Mediterranean sub-basins. Arrows illustrate the main pattern of present day surface circulation. Shaded areas mark the present day regions where intermediate and deep Mediterranean waters are formed.

density stratification which is less pronounced in the center than on the periphery.
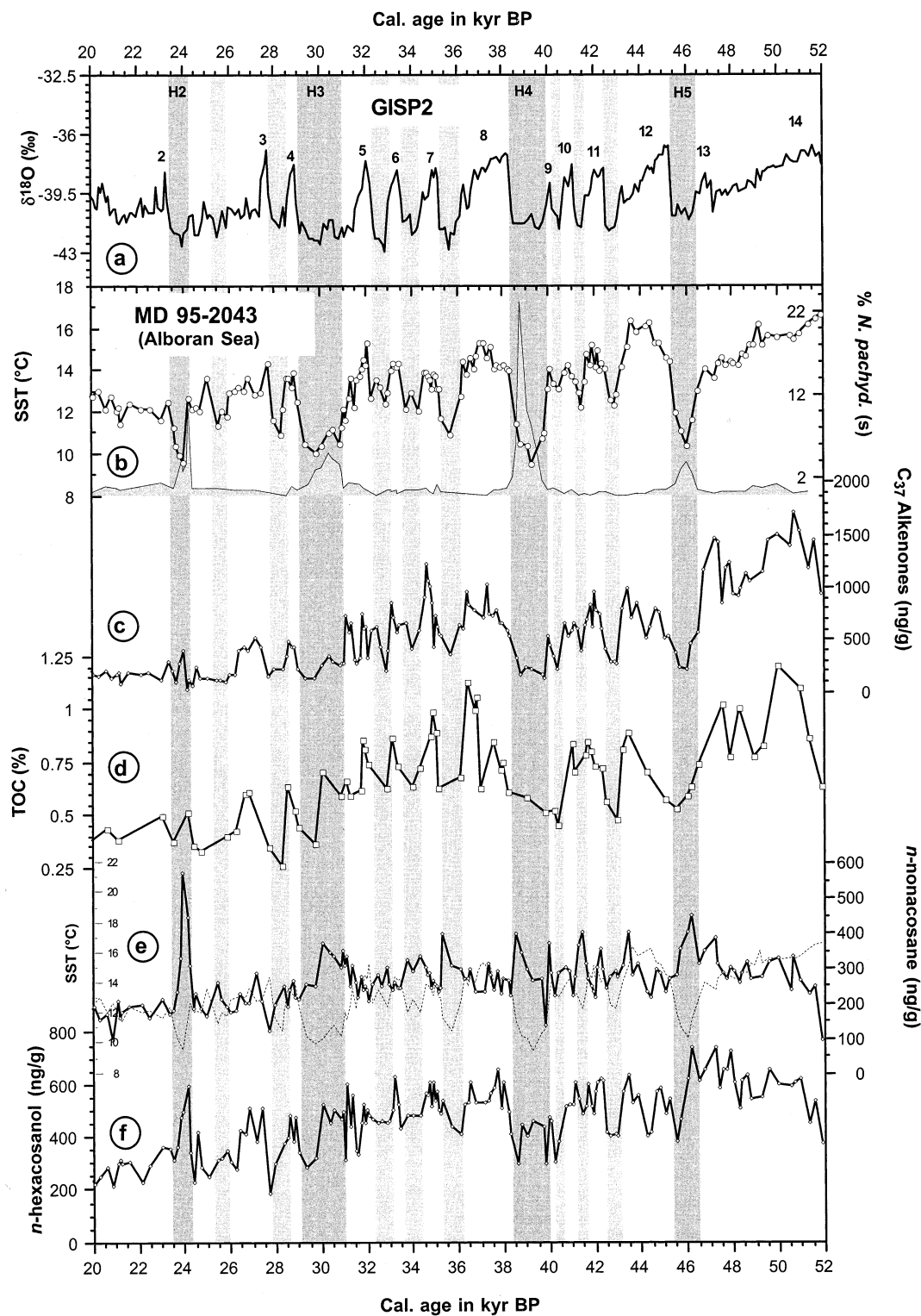
The intensity of north-westerlies over Europe depend on the Atlantic depressions. The Carcassone Cap (south-west of France), is the preferred southern route for these depressions, moving eastwards from the Atlantic to the Mediterranean region [18]. Westerlies blow through the passages between the Pyrenees, the Massif Central and the Alps, generating the local Tramontana and Mistral winds. These are strong airflows that may blow for several weeks in winter, carrying cold and dry polar or continental air masses to the Gulf of Lions [18,34]. They lead to strong evaporation and cooling of surface water which may become sufficiently dense to sink to a great depth. The production of relatively dense water can also occur sporadically over the wide continental shelf from the Gulf of Lions, although it does not contribute significantly to WMDW formation, since deep convection occurs in the offshore region of the gulf [31,34]. Thus, deep water formation was probably active too during glacial periods, when the sea level drop left most of the continental shelf in the Gulf of Lions above sea level.

Interannual variations in the formation rate of WMDW are associated with anomalies of the atmospheric forcing over the basin [20] giving rise to different types of deep water depending on predominant meteorological conditions [32]. Thus, WMDW formation has not been observed in years of relatively mild European winters, e.g. 1972. Results from circulation models indicate that wind stress determines the general circulation variability on the interannual time scale [35]. In addition, long meteorological and oceanographic time series show that the Mediterranean amplifies its circulation in response to the wind anomalies [35,36] which are the ultimate driving force for the main water flow through the straits of Sicily [37] and Gibraltar [36].

3. Materials and methods

Core MD 95-2043 was retrieved from the western Alboran Sea (36°8.6′N; 2°37.3′W; 1841 m water depth) during the 1995 IMAGES cruise onboard R/V Marion Dufresne. The chronological framework for the period covered in this study (20–52 kyr BP) is based on the correlation of the $U_{37}^{K'}$-SST profile with the $\delta^{18}O$ curve from GISP2 ice core [2,3]. This age model has been

previously presented and discussed, demonstrating that it does not introduce significant age modification in relation to another independent age model based on AMS ^{14}C ages and oxygen isotopic stratigraphy [5].

3.1. Molecular biomarkers

Three different molecular biomarkers are studied: long chain alkenones, alkanes and alcohols. All were analyzed using the same procedure. Sediment samples (≈ 2 g) were freeze-dried and manually grounded. After addition of an internal standard mixture containing n-nonadecan-1-ol, n-hexatriacontane and n-tetracontane, dry sediments were extracted in an ultrasonic bath with dichloromethane. The extracts were hydrolyzed with 6% potassium hydroxide in methanol for the elimination of wax ester interferences. Compounds were recovered with hexane and evaporated to dryness with an N_2 stream. The extracts were finally redissolved with toluene and derivatized with bis(trimethylsilyl)trifluoroacetamide before instrumental analysis.

The analyses were performed with a Varian gas chromatograph Model 3400 equipped with a septum programmable injector and a flame ionization detector. The instrument was equipped with a CPSIL-5 CB column coated with 100% dimethylsiloxane (film thickness 0.12 μm). Hydrogen was the carrier gas (50 cm/s). The oven temperature was programmed from 90° to 140°C at 20°C/min, then to 280°C at 6°C/min (holding time 25 min) and, finally, to 320°C at 10°C/min (holding time of 6 min). The injector was programmed from 90°C (holding time 0.3 min) to 320°C at 200°C/min (final holding time 55 min). Further details on the analytical conditions are given in [38]. Selected samples were examined by gas chromatography-mass spectrometry for confirmation of compound identification and evaluation of possible coelutions. The average reproducibility of the n-alkane, n-alcohol and alkenone concentrations was better than 10%. Five replicates of a sediment sample showed a standard deviation of ±0.15°C.

3.2. Total organic carbon (TOC)

Sediment samples for organic carbon were first freeze-dried and homogenized. The carbonate fraction was removed by addition of HCl solutions of increasing concentration, from 5 to 10%. The resulting suspension was centrifuged for 10–20 min at 3000 rpm to avoid loss of fine particles. Then the decarbonated sediment was neutralized by double washing with ultra-pure water and finally, freeze-dried. TOC was determined with a Carlo-Erba (NA 1500) Elemental Analyser and percentages calculated after correction for the carbonated fraction. Sample duplicates show a reproducibility better than 10%.

3.3. Carbon and oxygen isotopes

Stable isotope measurements were carried out on the planktic foraminifer *Globigerina bulloides* (25–30 well-preserved specimens picked from the 300–355 μm size) and on the benthic foraminifer *Cibicidoides* spp. (10–20 specimens picked from the 250–500 μm fraction). These measurements were made with a SIRA mass spectrometer equipped with a VG isocarb common acid bath system. Analytical reproducibility of laboratory standards was better than ±0.08‰ for $\delta^{18}O$. Calibration to VPDB is via the NBS19 standard.

4. Results

4.1. Organic matter records

The $U_{37}^{K'}$-SST profile from core MD 95-2043 for the last glacial period (Fig. 2b) has been shown

---

←

Fig. 2. (a) $\delta^{18}O$ profile from Greenland ice core GISP2 [2,3]. Numbers indicate the Dansgaard–Oeschger Interstadials and shaded bars show the position of the Stadials and HE2–5. (b–f) MD 95-2043 profiles of: (b) $U_{37}^{K'}$-SST (left axis), the thin line (right axis) shows the percentages of *N. pachyderma* [5]; (c) total C_{37} alkenone concentrations (marine); (d) total organic carbon (TOC) percentages; (e) n-nonacosane content (terrigenous, right axis), dotted line (left axis) is the same SST curve as in (b); (f) n-hexacosanol (terrigenous).

and discussed in a previous study [5] demonstrating its connection with the rapid climatic variability in Greenland ice cores [1–3]. The total amount of C_{37} alkenones (di-unsaturated plus tri-unsaturated C_{37} alkenones) shows also very strong oscillations along the glacial period (Fig. 2c). High values are recorded during the warm D–O Interstadials while the Stadials are well represented by drops in alkenone concentration. Minimum alkenone values are generally recorded during HE. The TOC profile, despite of its lower resolution, also shows large oscillations (0.6–1.2%) accompa-

nying the D–O cyclicity and, therefore, displays a great parallelism with the alkenone curve ($r = 0.86$, $P < 0.005$; Fig. 2d).

Terrestrial biomarkers, n-nonacosane and n-hexacosanol, also show a high short term variability along the glacial period (Fig. 2e,f). n-Nonacosane maxima correspond to cold periods, in opposition to C_{37} alkenones and TOC, reaching the highest values during H2 (Fig. 2e). In contrast, n-hexacosanol (Fig. 2f) does not show a clear pattern in relation to the D–O-type variability. Most of the warm intervals are associated
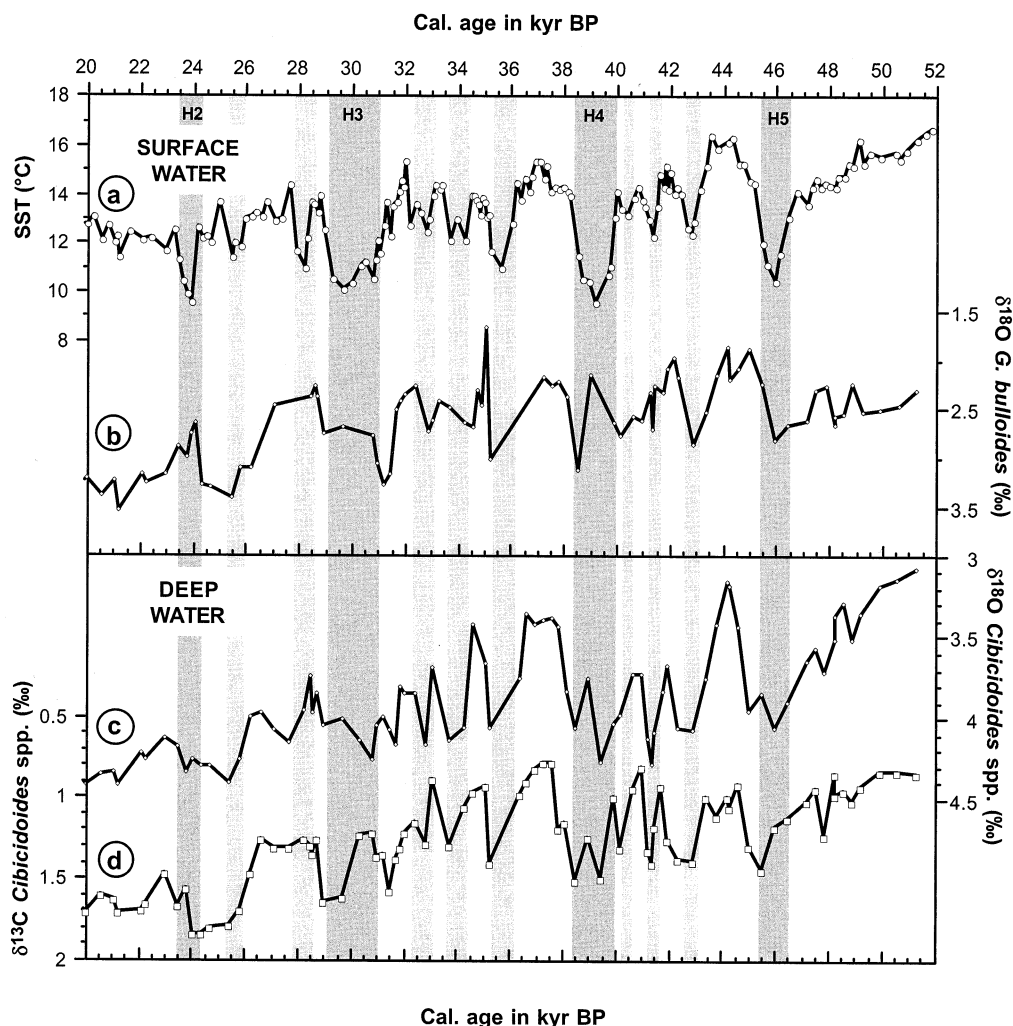

Fig. 3. MD 95-2043 age profiles of: (a) $U_{37}^{K'}$-SST; (b) $\delta^{18}O$ *G. bulloides* (reverse *y* axis); (c) $\delta^{18}O$ *Cibicidoides* spp. (reverse *y* axis); (d) $\delta^{13}C$ *Cibicidoides* spp. (reverse *y* axis).

with higher values than the cold intervals, although this difference is not always well defined. The lower parallelism between the two terrestrial proxies ($r = 0.6$, $P < 0.005$) reflects a complex behavior suggesting that other factors, independent of the terrestrial input, modulate the terrigenous sedimentary signal.

4.2. Isotopic records

The $\delta^{18}O$ record from *G. bulloides* (Fig. 3b) exhibits ($\sim 1\permil$) depletions and enrichments associated with the D–O Interstadials and Stadials, respectively. These isotopic enrichments are less defined during the Stadials which are associated with a HE, probably as consequence of the entrance, during these period, of fresh melt polar water through the Strait of Gibraltar [5]. The two, $\delta^{18}O$ and $\delta^{13}C$, benthic isotopic curves (Fig. 3c,d) show a great parallelism ($r = 0.86$, $P < 0.005$) recording high and low values during Stadials and Interstadials respectively. The D–O-type variability in *Cibicidoides* spp. $\delta^{18}O$ (0.5–$1\permil$) is clearer than in *G. bulloides* $\delta^{18}O$ since the isotopic enrichment in the deep waters is well defined for all the Stadial periods, even those coincident with HE. The intensity of the benthic $\delta^{13}C$ oscillations related to the D–O cycles was about $0.6\permil$, and consequently larger than the mean deep ocean $\delta^{13}C$ enrichment ($0.46\permil$) associated with the last deglaciation [39]. *Cibicidoides* spp. are epibenthic species and their $\delta^{13}C$ composition is dominated by deep water ventilation conditions [40–42]. The low values recorded during the Interstadials (0.8–$1\permil$) indicate that the deep water masses were not well ventilated during these episodes although they never reached anoxic values.
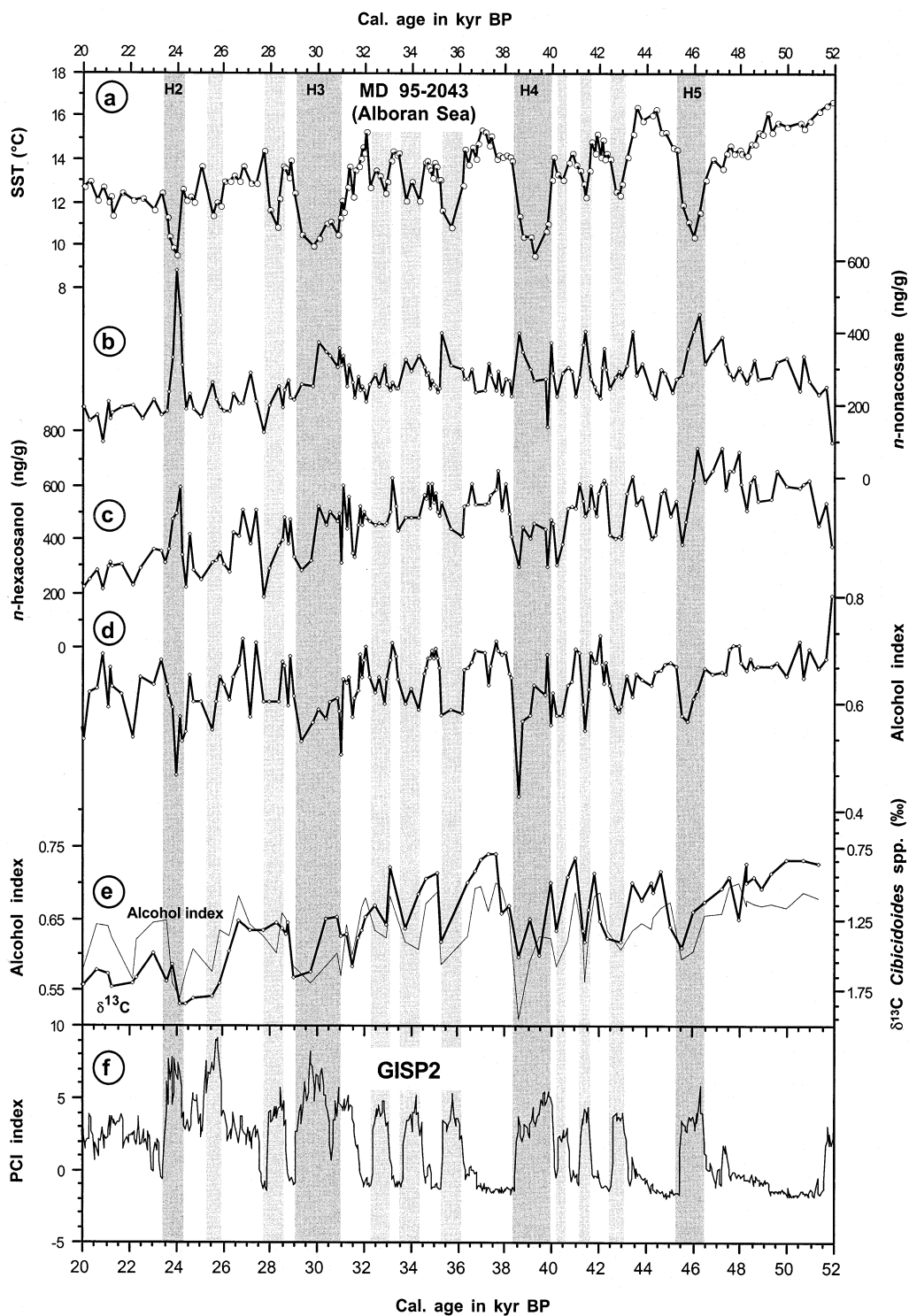
5. Discussion

5.1. Changes in western Mediterranean deep water conditions

The D–O-type variability recorded in both benthic $\delta^{18}O$ and $\delta^{13}C$ profiles (Fig. 3c,d) monitors the same oceanographic process consisting of the formation of a denser (higher $\delta^{18}O$ values) and better ventilated (higher $\delta^{13}C$ values) deep water mass during the Stadials than during the Interstadials. It can be therefore inferred that changes in the glacial WMDW properties occurred in parallel with the D–O oscillations. This glacial WMDW should be formed in the Gulf of Lions (north-western Mediterranean) analogously to the present day WMDW circulation pattern (cf. Section 2). As indicated above, winter westerly winds are one of the main forcing factors of this process and their strength is related to the presently observed interannual variability in the intensity of WMDW formation [35,43].

The high *n*-nonacosane values (Fig. 2e) recorded during the cold Stadials also suggest the occurrence of enhanced wind transport in agreement with the proposed westerly wind-meditated teleconnection between the Mediterranean Sea and Greenland during these cold intervals [5,44]. The higher intensity of the north Hemisphere wind system during the Stadials is also documented by dust records in Greenland [45], loess deposits in the Chinese Plateau and salinity oscillations in the south China Sea [46,47]. In addition to these stronger winds the climatic conditions over the Mediterranean region may also have favored higher water evaporation assisting WMDW formation. Evidence of increased evaporation is obtained from pollen records from the Laghi di Monticchio (south Italy) showing the occurrence of more arid conditions during the Stadials and especially HE than during the Interstadials [48]. Climatic conditions over the eastern Mediterranean Sea could also help the formation of WMDW by the production of a denser LIW during these cold intervals.

The differences observed between the two terrestrial biomarkers can be evaluated by examination of the *n*-hexacosanol/(*n*-nonacosane+*n*-hexacosanol) index. This alcohol index (Fig. 4d) evolves in parallel with the SST record ($r = 0.75$, $P < 0.005$) displaying low and high values during Stadials and Interstadials, respectively. Changes in vegetation type have been reported to be associated with chain length of the homologous biomarker distributions [49,50] whereas the relative content in *n*-alkan-1-ol vs. *n*-alkanes seems to be

more related to sedimentary conditions since the former are more labile to degradation processes than the latter. Thus, organic matter degradation decreases n-alcohol abundance in relation to n-alkanes lowering the alcohol index. Recently, n-alcohol vs. n-alkane rate changes have been interpreted to record organic matter degradation rates in the water column [51–53]. However, alcohol indices were found to differ between sapropelic and non-sapropelic layers of the eastern Mediterranean being interpreted to relate to eolian-fluvial transport [54].

Further insight into the significance of this alcohol index in the Alboran Sea can be obtained by comparison with the $\delta^{13}C$ record. As sampling resolution between the two curves is very different, the resolution of the index has been lowered to that of $\delta^{13}C$ (Fig. 4e). Both curves evolve in parallel ($r = 0.74$, $P < 0.005$) suggesting a common forcing mechanism in agreement with degradation rate oscillations of the organic matter driven by deep water ventilation conditions. n-Hexacosanol preservation was drastically affected by ventilation changes while the n-nonacosane profile keeps better the original signal of terrestrial input.

A polar circulation index (PCI) was calculated by examination of sea salt and dust series from GISP2 core [55]. The time evolution of this PCI is interpreted to reflect the combined intensity and overall size of the circulation system that produces the well-mixed background atmosphere over Greenland. Comparison of PCI and alcohol indices (Fig. 4) shows a good inverse correlation ($r = 0.75$, $P < 0.005$) which is again consistent with the north Hemisphere wind system as the major factor controlling deep water ventilation and preservation of the organic matter in the western Mediterranean Sea.

Downcore concentrations of TOC and C_{37} alkenones are usually interpreted as a paleoproductivity signal [12–14]. Nevertheless, they can be also strongly affected by degradation processes in the water column and sediment [56]. Both C_{37} alkenones and TOC (Fig. 2c,d) in core MD 95-2043 show the same pattern as the alcohol index (correlation index $r = 0.76$ and $r = 0.66$ ($P < 0.005$ in both cases) for the C_{37} alkenones and TOC, respectively). This parallelism is in agreement with the dominance of a preservation signal for these two records in the deep Alboran Sea. Nevertheless, it cannot be excluded that increased phytoplanktonic activity during the D–O Interstadials may also contribute to the higher TOC and alkenone values recorded during these periods. Additional proxies, not affected by changes in deep water ventilation, are necessary for further assessment on possible changes in biological activity.

5.2. Implications for the Mediterranean thermohaline circulation variability

The results of core MD 95-2043 document an enhanced Mediterranean thermohaline circulation during both the HE and the rest of D–O Stadials in comparison to the warm intervals (Fig. 5). This scenario is opposite to that described for the north Atlantic Ocean, where both benthic $\delta^{13}C$ and foraminiferal assemblage records indicate a reduced deep water ventilation during the cold D–O intervals [57–59]. A more intense Mediterranean deep water overturning must be concurrent with increased water exchange through the Gibraltar Strait, implying the reinforcement of the dense Mediterranean water outflow towards the Atlantic Ocean.

Present day MOW spreads westwards, deepening into the Atlantic Ocean until it becomes neutrally buoyant at intermediate depths (800–1300 m) [60,61]. The MOW forms a salt tongue along the coast of Portugal, extending as far as the Bermuda rise [61]. Since MOW is one of the salt-contributing members to the north Atlantic deep water (NADW) it has been postulated that it may significantly influence Atlantic overturning [61,62]. However, despite the important effect of MOW in the salt budget of the Atlantic, simula-

←

Fig. 4. MD 95-2043 age profiles of: (a) $U^{K'}_{37}$-SST; (b) n-nonacosane; (c) n-hexacosanol; (d) alcohol index: n-hexacosanol/(n-hexacosanol+n-nonacosane); (e) $\delta^{13}C$ *Cibicidoides* spp. (thick line) and alcohol index (thin line) with the same sampling resolution as the $\delta^{13}C$ *Cibicidoides* spp. curve; (f) polar circulation index (PCI) in GISP2 ice core [55].

Heinrich Events & Dansgaard-Oeschger Stadials
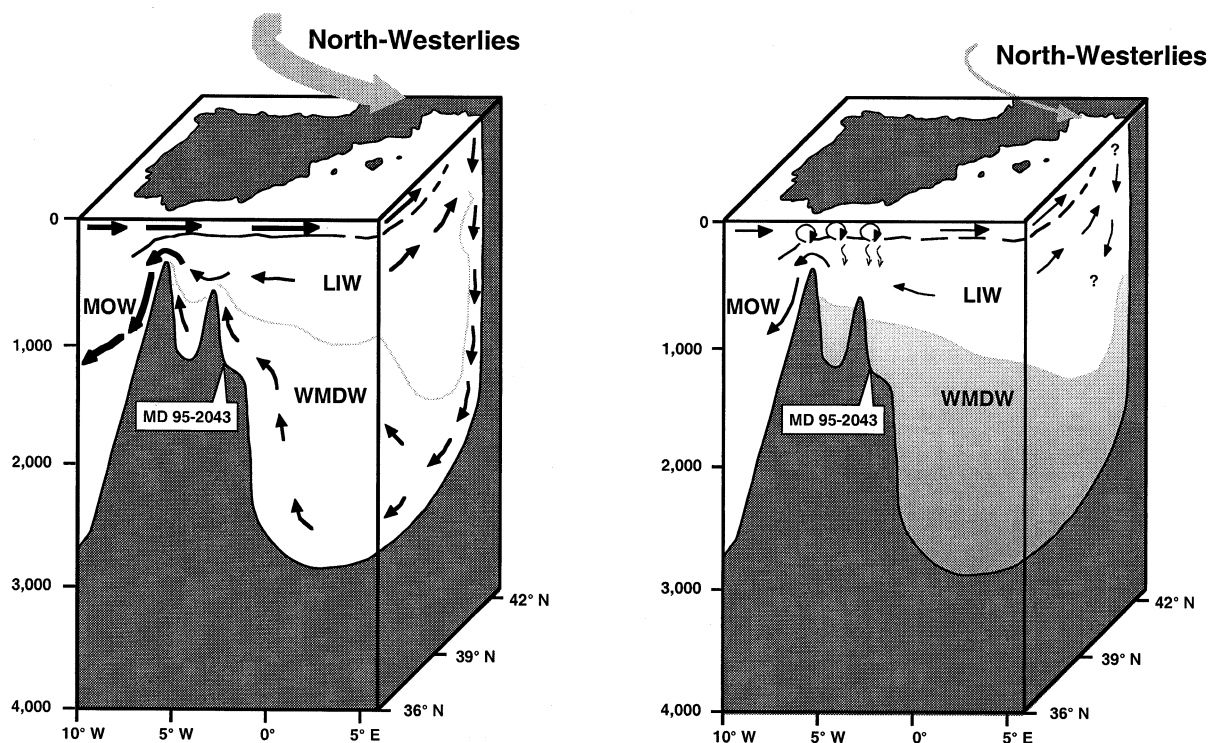
Dansgaard-Oeschger Interstadials

Fig. 5. Illustration of the hypothesized processes controlling the studied records in core MD 95-2043 during the cold HE and D–O Stadials (a) and during the warm D–O Interstadials (b).

tions with a circulation model indicate that it has little effect on the global ocean thermohaline circulation [63]. In any case, given the opposite situations regarding deep water formation in the Atlantic and Mediterranean during glacial times, it could be hypothesized that MOW had a stronger role during cold intervals, when MOW was enhanced and the Atlantic thermohaline circulation was drastically reduced.

Positive benthic δ^{13}C anomalies associated with last glacial maximum (LGM) intermediate waters have been found in the Gulf of Cadiz, north-western African margin [64], along the Portuguese continental slope, in the Gulf of Gascogne [65] and in the Caribbean Sea [66]. Therefore, it was postulated that the glacial MOW was more important in the intermediate Atlantic than it is to-

day [64]. Nevertheless, this view is controversial since MOW volume had to be reduced during the glacial sea level drop (~ 120 m) [29,65,67]. Furthermore, sediment records and simulations with an ocean circulation-biogeochemical model suggest that the north Atlantic still remained an important source of intermediate water during the LGM [68,69]. The LGM high δ^{13}C values in the Caribbean Sea and Iberian margin have also been associated with a well-ventilated and nutrient-depleted glacial north Atlantic intermediate water [70]. Close comparison of our benthic δ^{13}C record in the Alboran Sea (Fig. 2d) with core SO75-26KL in the Portuguese margin [70] shows clearly opposite trends during H2 and H4. This supports the hypothesis of a strong reduction of Atlantic intermediate water ventilation during HE without

significant influence from the well-ventilated MOW [70].

6. Conclusions

Sedimentary profiles from both terrestrial and marine biomarkers, TOC and benthic isotopes in the Alboran Sea were modulated by a D–O-type variability between 20–50 kyr BP. The benthic $\delta^{18}O$ and $\delta^{13}C$ records document the occurrence of a denser and better ventilated deep water mass during the HE and D–O Stadials than during the warm D–O Interstadials. This is also illustrated by the *n*-hexadecanol/*n*-nonadecane index, reflecting that in conditions of well-ventilated deep water (cold intervals) organic matter degradation processes were enhanced. In consequence, TOC and C_{37} alkenones are also modulated by these changes in preservation conditions although the influence of enhanced primary productivity during the warm intervals cannot be completely ruled out.

This denser water mass likely resulted from enhanced thermohaline circulation in the northwestern Mediterranean Sea by the intensification of north-westerlies which today constitute the major driving force for deep water formation in this area (Fig. 5). Increased wind transport occurring synchronously with deep water formation can also be inferred from the *n*-nonacosane record. This association is also consistent with the high correlation between our profiles reflecting deep water ventilation proxies and the PCI in Greenland, an indicator of the atmospheric conditions at higher latitudes (Fig. 4).

Acknowledgements

References

[1] W. Dansgaard, S. Johnsen, H.B. Clausen, D. Dahl-Jensen, N.S. Gundestrup, C.U. Hammer, C.S. Hvidberg, J.P. Steffensen, A.E. Sveinbjörnsdottir, J. Jouzel, G. Bond, Evidence for general instability of past climate from a 250-kyr ice-core record, Nature 364 (1993) 218–220.

[2] P.M. Grootes, M. Stuiver, J.W.C. White, S. Johnsen, J. Jouzel, Comparison of oxygen isotope records from the GISP2 and GRIP Greenland ice cores, Nature 366 (1993) 552–554.

[3] D.A. Meese, A.J. Gow, R.B. Alley, G.A. Zielinski, P.M. Grootes, The Greenland Ice Sheet Project 2 depth-age scale: Methods and results, J. Geophys. Res. 102 (1997) 26411–26423.

[4] J.P. Sachs, S.J. Lehman, Subtropical north Atlantic temperatures 60,000 to 30,000 years ago, Science 286 (1999) 756–759.

[5] I. Cacho, J.O. Grimalt, C. Pelejero, M. Canals, F.J. Sierro, J.A. Flores, N.J. Shackleton, Dansgaard-Oeschger and Heinrich event imprints in the Alboran Sea paleotemperatures, Paleoceanography 14 (1999) 698–705.

[6] I.L. Hendy, J.P. Kennett, Dansgaard-Oeschger cycles and the California Current System: Planktonic foraminiferal response to rapid climate change in Santa Barbara Basin, Ocean Drilling Program hole 893A, Paleoceanography 15 (2000) 30–42.

[7] J.P. Béthoux, Budgets of the Mediterranean Sea. Their dependence on the local climate and on the characteristics of the Atlantic waters, Oceanol. Acta 2 (1979) 157–163.

[8] H. Lacombe, J.C. Gascard, J. Cornella, J.P. Béthoux, Response of the Mediterranean to the water and energy fluxes across its surface, on seasonal and interannual scales, Oceanol. Acta 4 (1981) 247–255.

[9] R. von Grafenstein, R. Zahn, R. Tiedeman, A. Murat, Planktonic $\delta^{18}O$ record at sites 976 and 977, Alboran Sea: stratigraphy, forcing, and paleoceanographic implications, in: R. Zahn, M.C. Comas, A. Klaus (Eds.), Proc. Ocean Drill. Prog. Sci. Res. 161 (1999) 469–479.

[10] J.K. Volkman, G. Eglinton, E.D.S. Corner, T.E.V. Forsberg, Long-chain alkenes and alkenones in the marine coccolitophorid *Emiliania huxleyi*, Phytochemistry 19 (1980) 2619–2622.

[11] I.T. Marlowe, S.C. Brassell, G. Eglinton, J.C. Green, Long-chain alkenones and alkyl alkenoates and the fossil

coccolith record of marine sediments, Chem. Geol. 88 (1990) 349–375.

[12] R.R. Schneider, P.J. Müller, G. Ruhland, G. Meinecke, H. Schmidt, G. Wefer, Late Quaternary surface temperatures and productivity in the East-Equatorial South Atlantic: response to changes in trade/monsoon wind forcing surface water advection, in: G. Wefer, W.H. Berger, G. Siedler, D.J. Webb (Eds.), The South Atlantic: Present and Past Circulation, Springer, Berlin, 1996, pp. 527–551.

[13] J. Villanueva, J.O. Grimalt, L.D. Labeyrie, E. Cortijo, L. Vidal, J.L. Turon, Precessional forcing of productivity in the North Atlantic Ocean, Paleoceanography 13 (1998) 561–571.

[14] S. Schulte, F. Rostek, E. Bard, J. Rullkötter, O. Marchal, Variations of oxygen-minimum and primary productivity recorded in sediments of the Arabian Sea, Earth Planet. Sci. Lett. 173 (1999) 205–221.

[15] G. Eglinton, R.J. Hamilton, Leaf epicuticular waxes, Science 156 (1967) 1322–1335.

[16] L.A.S. Madureira, S.A. van Kreveld, G. Eglinton, M.H. Conte, G.M. Ganssen, J.E. van Hinte, J.J. Ottens, Late Quaternary high-resolution biomarker and other sedimentary climate proxies in a northeast Atlantic core, Paleoceanography 12 (1997) 255–269.

[17] J. Villanueva, J.O. Grimalt, E. Cortijo, L. Vidal, L.D. Labeyrie, A biomarker aproach to the organic matter deposited in the North Atlantic during the Last climatic cycle, Geochim. Cosmochim. Acta 61 (1997) 4633–4646.

[18] R.G. Barry, R.J. Chorley, Atmosphere, Weather and Climate, Routledge, London, 1998, 409 pp.

[19] J.P. Béthoux, Mean water fluxes across sections in the Mediterranean Sea, evaluated in the basis of water and salt budgets and of observed salinities, Oceanol. Acta 3 (1980) 79–88.

[20] N. Pinardi, E. Masetti, Variability of the large scale general circulation of the Mediterranean Sea from observations and modelling: a review, Palaeogeogr. Palaeoclimatol. Palaeoecol. 158 (2000) 153–173.

[21] P.E. La-Violette, Short-term measurements of surface currents associated with the Alboran Sea Gyre, J. Phys. Oceanogr. 16 (1986) 262–279.

[22] R.E. Cheney, R.A. Doblar, Structure and variability of the Alboran frontal system, J. Geophys. Res. 87 (C1) (1982) 585–594.

[23] J. Candela, C.D. Winant, H.L. Bryden, Meteorological forced subinertial flows through the Strait of Gibraltar, J. Geophys. Res. 94 (C9) (1989) 12667–12679.

[24] H. Perkins, T. Kinder, P. La-Violette, The Atlantic inflow in the Western Alboran Sea, J. Phys. Oceanogr. 20 (1990) 242–263.

[25] G.W. Heburn, P.E. La-Violette, Variations in the structure of the anticyclonic gyres found in the Alboran Sea, J. Geophys. Res. 95 (C2) (1990) 1599–1613.

[26] G. Parrilla, T.H. Kinder, R.H. Preller, Deep and Intermediate Mediterranean Water in the Western Alboran Sea, Deep Sea Res. 33 (1986) 55–88.

[27] J. Font, The path of the Levantine Intermediate Water to the Alboran Sea, Deep Sea Res. 34 (1987) 1745–1755.

[28] P. Pistek, F. de-Strobel, C. Montanari, Deep sea circulation in the Alboran Sea, J. Geophys. Res. 90 (C3) (1985) 4969–4976.

[29] H.L. Bryden, H.M. Stommel, Limiting processes that determine basic features of the circulation in the Mediterranean Sea, Oceanol. Acta 7 (1984) 289–296.

[30] T.H. Kinder, G. Parrilla, Yes, some of the Mediterranean outflow does come from great depth, J. Geophys. Res. 92 (C3) (1987) 2901–2906.

[31] MEDOC-Group, Observations of formation of deep water in the Mediterranean Sea, 1969, Nature 227 (1970) 1037–1040.

[32] H. Lacombe, P. Tchernia, L. Gamberoni, Variable bottom water in the Western Mediterranean Basin, Progr. Oceanogr. 14 (1985) 319–338.

[33] K.D. Leaman, F.A. Schott, Hydrographic structure of the convection regime in the Gulf of Lions: Winter 1987, J. Phys. Oceanogr. 21 (1991) 575–598.

[34] C. Millot, The Gulf of Lions hydrodynamics, Cont. Shelf Res. 10 (1990) 885–894.

[35] G. Korres, N. Pinardi, A. Lascaratos, The ocean response to low frequency interannual atmospheric variability in the Mediterranean Sea. Part I: Sensitivity experiments and energy analysis, J. Clim. 13 (2000) 705–731.

[36] M. Astraldi, G.P. Gasparini, The seasonal characteristics of the circulation in the North Mediterranean basin and their relationship with the atmospheric-climatic conditions, J. Geophys. Res. 97 (C6) (1992) 9531–9540.

[37] G.M.R. Manzella, G.P. Gasparini, M. Astraldi, Water exchange between the eastern and the western Mediterranean through the Strait of Sicily, Deep Sea Res. 35 (1988) 1021–1035.

[38] J. Villanueva, C. Pelejero, J.O. Grimalt, Clean-up procedures for the unbiased estimation C_{37} alkenone sea surface temperatures and terrigenous n-alkane inputs in paleoceanography, J. Chromatogr. A 757 (1997) 145–151.

[39] W.B. Curry, J.C. Duplessy, L.D. Labeyrie, N.J. Shackleton, Changes in the distribution of $\delta^{13}C$ of deep water δCO_2 between the last glaciation and the Holocene, Paleoceanography 3 (1988) 317–341.

[40] J.C. Duplessy, N.J. Shackleton, R.K. Matthews, W.L. Prell, W.F. Ruddiman, M. Caralp, C. Hendy, ^{13}C record of benthic foraminifera in the last interglacial ocean: implications for the carbon cycle and the global deep water circulation, Quat. Res. 21 (1984) 225–243.

[41] R. Zahn, K. Winn, M. Sarnthein, Benthic foraminiferal $\delta^{13}C$ and accumulation rates of organic carbon: *Uvigerina peregrina* group and *Cibicidoides wuellerstorfi*, Paleoceanography 1 (1986) 27–42.

[42] A.V. Altenbach, M. Sarnthein, Productivity record in benthic foraminifera, in: W.H. Berger, V.S. Smetacek, G. Wefer (Eds.), Productivity of the Ocean: Past and Present, John Wiley, New York, 1989, pp. 255–269.

[43] F. Schott, K.D. Leaman, Observations with moored acoustic doppler current profiles in the convection regime

in the Golfe du Lion, J. Phys. Oceanogr. 21 (1991) 558–574.

[44] E.J. Rohling, A. Hayes, S. De Rijk, D. Kroon, W.J. Zachariasse, D. Eisma, Abrupt cold spells in the northwest Mediterranean, Paleoceanography 13 (1998) 316–322.

[45] K.C. Taylor, G.W. Lamorey, G.A. Doyle, R.B. Alley, P.M. Grootes, P.A. Mayewski, J.W.C. White, L.K. Barlow, The 'flickering switch' of late Pleistocene climate change, Nature 361 (1993) 432–436.

[46] F.H. Chen, J. Blomendal, J.M. Wang, J.J. Li, F. Oldfield, High-resolution multi-proxy climate records from Chinese loess: evidence for rapid climatic changes over the last 75 kyr, Palaeogeogr. Palaeoclimatol. Palaeoecol. 130 (1997) 323–335.

[47] L. Wang, T. Oba, Tele-connections between East Asian monsoon and the high-latitude climate: A comparison between the GISP2 Ice Core Record and the high resolution marine records from the Japan and South China Seas, Quat. Res. 37 (1998) 211–219.

[48] W.A. Watts, J.R.M. Allen, B. Huntley, Vegetation history and paleoclimate of the last glacial period at lago grande di Monticchio, southern Italy, Quat. Sci. Rev. 15 (1996) 133–153.

[49] R.B. Gagosian, E.T. Peltzer, J.T. Merrill, Long-range transport of terrestrially derived lipids in aerosols from the South Pacific, Nature 325 (1987) 800–803.

[50] J.G. Poynter, P. Farrimond, N. Robinson, G. Eglinton, Aeolian-derived higher plant lipids in the marine sedimentary record: Links with palaeoclimate, in: M. Leinen, M. Sarnthein (Eds.), Paleoclimatology and Paleometeorology: Modern and Past Patterns of Global Atmospheric Transport, Kluwer Academic Publishers, Dordrecht, 1989, pp. 435–462.

[51] J. Poynter, G. Eglinton, Molecular composition of three sediments from hole 717C: The Bengal fan, Proc. Ocean Drill. Prog. Sci. Res. 116 (1990) 155–161.

[52] L. Westerhausen, J. Poynter, G. Eglinton, H. Erlenkeuser, M. Sarnthein, Marine and terrigenous origin of organic matter in the modern sediments of the equatorial East Atlantic: the $\delta^{13}C$ and molecular record, Deep Sea Res. 40 (1993) 1087–1121.

[53] V. Santos, D.S.M. Billett, A.L. Rice, G.A. Wolff, Organic matter in deep-sea sediments from the Porcupine Abyssal Plain in the North-east Atlantic Ocean. I-Lipids, Deep Sea Res. 41 (1994) 787–819.

[54] H.L. ten-Haven, M. Baas, J.W. De-Leeuw, P.A. Schenck, H. Brinkhuis, Late Quaternary Mediterranean sapropels. II. Organic geochemistry and palynology of S1 sapropels and associated sediments, Chem. Geol. 64 (1987) 149–167.

[55] P.A. Mayewski, L.D. Meeker, S. Whitlow, M.S. Twickler, M.C. Morrison, P. Bloomfield, G.C. Bond, R.B. Alley, A.J. Gow, P.M. Grootes, D.A. Meese, M. Ram, K.C. Taylor, W. Wumkes, Changes in atmospheric circulation and ocean ice cover over the North Atlantic during the last 41,000 years, Science 263 (1994) 1747–1751.

[56] F.G. Prahl, G.J.D. Lange, M. Lyle, M.A. Sparrow, Post-depositional stability of long-chain alkenones under contrasting redox conditions, Nature 341 (1989) 434–437.

[57] T.L. Rasmussen, E. Thomsen, L.D. Labeyrie, T.C.E.v. Weering, Circulation changes in the Faeroe-Shetland channel correlating with cold events during the last glacial period (58–10 ka), Geology 24 (1996) 937–940.

[58] W.B. Curry, D.W. Oppo, Synchronous, high-frequency oscillations in tropical sea surface temperatures and North Atlantic Deep Water production during the last glacial cycle, Paleoceanography 12 (1997) 1–14.

[59] L. Vidal, L.D. Labeyrie, E. Cortijo, M. Arnold, J.C. Duplessy, E. Michel, S. Becqué, T.C.E. Van Weering, Evidence for changes in the North Atlantic Deep Waters linked to meltwater surges during the Heinrich events, Earth Planet. Sci. Lett. 146 (1997) 13–27.

[60] J.F. Prices, M.O.N. Baringer, R.G. Lueck, G.C. Johnson, I. Ambar, G. Parrilla, A. Cantos, M.A. Kennelly, T.B. Sanford, Mediterranean outflow mixing and dynamics, Science 259 (1993) 1277–1282.

[61] M.O.N. Baringer, J.F. Prices, A review of the physical oceanography of the Mediterranean outflow, Mar. Geol. 155 (1999) 63–82.

[62] J.L. Reid, On the contribution of the Mediterranean Sea outflow to the Norwegian-Greenland Sea, Deep Sea Res. 26A (1979) 1199–1223.

[63] D.G. Wright, T.F. Stocker, Sensitivities of a zonally averaged global ocean circulation model, J. Geophys. Res. 97 (C8) (1992) 12707–12730.

[64] R. Zahn, M. Sarnthein, H. Erlenkeuser, Benthic isotope evidence for changes of the Mediterranean outflow during the late Quaternary, Paleoceanography 2 (1987) 543–559.

[65] J.C. Duplessy, N.J. Shackleton, R.G. Fairbanks, L. Labeyrie, D. Oppo, N. Kallel, Deepwater source variations during the last climatic cycle and their impact on the global deepwater circulation, Paleoceanography 3 (1988) 343–360.

[66] D.W. Oppo, R.G. Fairbanks, Variability in the deep and intermediate water circulation of the Atlantic Ocean during the past 25,000 years: Northern Hemisphere modulation of the Southern Ocean, Earth Planet. Sci. Lett. 86 (1987) 1–15.

[67] J.P. Béthoux, Paléo-hydrologie de la Méditerranée au cours des derniers 20000 ans, Oceanol. Acta 7 (1984) 43–48.

[68] D.W. Oppo, S.J. Lehman, Mid-depth circulation of the subpolar North Atlantic during the last glacial maximum, Science 259 (1993) 1148–1152.

[69] O. Marchal, T.F. Stocker, F. Joos, Impact of oceanic reorganizations on the ocean carbon cycle and atmospheric carbon dioxide content, Paleoceanography 13 (1998) 225–244.

[70] R. Zahn, J. Schönfeld, H.-R. Kudrass, M.-H. Park, H. Erlenkeuser, P.M. Grootes, Thermohaline instability in the North Atlantic during meltwater events: Stable isotope and ice-rafted detritus records from core SO75-26KL, Portuguese margin, Paleoceanography 12 (1997) 696–710.